Chapter 5

A Phase Change Problem including Space-Dependent Latent Heat and Periodic Heat Flux

5.1 Introduction

In recent years, phase-change problem (Stefan problem) involving diffusion process and variable latent heat is of great interest from mathematical and physical points of views. The work related to diffusion process and its occurrence can be found in many aspects of research (Ouedraogo et al., 2008; Raheem, 2013; Chhetri and Vatsala, 2018). Physically, variable latent heat term arises in the Stefan problem governing the processes of movement of a shoreline in a sedimentary ocean basin due to changes in various parameters (Voller et al., 2004). Some solutions of Stefan problems including space-dependent latent heat have been reported in Rajeev et al. (2009a), Rajeev et al. (2013), Rajeev (2014). Zhou et al. (2014) presented a phase change model (Stefan problem) that contains variable latent heat term and they discussed the similarity solution to the problem. After that Zhou and Xia (2015) used the Kummer functions to present similarity solution to a Stefan problem containing a more general variable latent heat term. Mathematically, Stefan problem with periodic boundary are always interested due to the difficulty associated with its solution. From the literature, it is found that the exact solution to the phase-change problem with periodic heat-flux is not known even in its simplest form and a sophisticated scheme is required to solve these problems (Rizwan-Uddin, 1999). Therefore, various numerical

(Rizwan-Uddin, 1998; Savovic and Caldwell, 2003; Ahmed, 2006) and approximate analytical techniques (Rajeev et al., 2009b; Rajeev, 2014) have been used by the researchers to solve the phase-change problem containing the boundary conditions of periodic nature.

In this study, we consider a Stefan problem containing space dependent latent heat and a periodic boundary condition. The solution of the problem is obtained by a well-known approximate technique homotopy analysis technique introduced by Liao (1997). From the literature (Liao, 2009; Abbasbandy, 2006; Gorder and Vajravelu, 2009; Zahran, 2009; Jafary et al., 2010; Onyejekwe, 2014), it can be seen that this scheme is used by many researchers to solve various problems occurring in science and industries. In this chapter, Wolfram Mathematica 8.0.1 has been used for all the computations with the aid of Stavroulakis and Tersian (2004). For the validity of proposed solution, the comparisons have been made with the analytical solution in a particular case. Dependence of movement of interface on some parameters is also analysed.

5.2 Mathematical Formulation

This section presents a phase-change problem involving melting/freezing process in the half plane, i.e. $x > 0$. Motivated by the work of Zhou et al. (2014) and Zhou and Xia (2015), we have assumed that the latent heat is space dependent. Moreover, a periodic surface heat flux is supposed in the problem. The mathematical model describing the process is given below:

$$\frac{\partial T}{\partial t} = \alpha \frac{\partial^2 T}{\partial x^2}, \qquad 0 < x < s(t),\ t > 0, \tag{5.1}$$

$$T(s(t),t) = 0, \qquad t > 0, \tag{5.2}$$

$$k\frac{\partial T(0,t)}{\partial x} = -q(1+\in \sin \omega t) \,, \tag{5.3}$$

$$k\frac{\partial T(s(t),t)}{\partial x} = -\gamma\, s\frac{ds}{dt} \,, \tag{5.4}$$

$$s(0) = 0 \,, \tag{5.5}$$

where $T(x,t)$ is the temperature profile, x represents the space variable, t is the time, α denotes the thermal diffusivity, $s(t)$ denotes the tracking of moving phase front, k is the thermal conductivity, ω is oscillation frequency, $\in$ is the amplitude, $q(1+\in \sin \omega t)$ is the periodic heat flux and $\gamma\, s$ is latent heat term per unit volume which depends on space.

5.3 Solution of the Problem

According to the HAM (Liao, 2009; Abbasbandy, 2006), we assume

$$N[\phi(x,t;p)] = \frac{\partial}{\partial t}\phi(x,t;p) - \alpha\frac{\partial^2}{\partial x^2}\phi(x,t;p) \tag{5.6}$$

and

$$L[\phi(x,t;p)] = \frac{\partial^2}{\partial x^2}\phi(x,t;p) \,, \tag{5.7}$$

as the non-linear and linear operators, respectively.

For Eq. (5.1), we first construct the following homotopy:

$$(1-p)\,L[\phi(x,t;p) - T_0(x,t)] = p\mu\, H(x,t)N[\phi(x,t;p)] \,, \tag{5.8}$$

where $p \in [0,1]$ denotes the embedding parameter, $T_0(x,t)$ represents the initial guess, $\mu \neq 0$ is the auxiliary parameter, $H(x,t) \neq 0$ is the auxiliary function.

If we substitute $p=0$ and $p=1$ in Eq. (5.8) then we simply obtain $\phi(x,t;0)=T_0(x,t)$ and $\phi(x,t;1)=T(x,t)$, respectively. This indicates that when p tends 1 from 0, the initial estimate $T_0(x,t)$ shifts towards $T(x,t)$ which satisfies the proposed problem.

For Eq. (5.1), we can get the *m*-th order deformation equation (Liao, 2009; Abbasbandy, 2006) as given below:

$$L[T_m(x,t)-\chi_m T_{m-1}(x,t)]=\mu H(x,t)R_m(\overline{T}_{m-1}), \tag{5.9}$$

where $R_m(\overline{T}_{m-1})=\dfrac{\partial T_{m-1}(x,t)}{\partial t}-\alpha\dfrac{\partial^2 T_{m-1}(x,t)}{\partial x^2}$

and $\chi_m=\begin{cases}0, & m<2\\ 1, & m\geq 2\end{cases}$.

According to Rajeev et al. (2013), we consider the following initial approximation of $T(x,t)$:

$$T_0(x,t)=\frac{q}{k}\left((1+\in\sin\omega t)(s_0-x)\right), \tag{5.10}$$

where $s_0=\left(\dfrac{2q}{\gamma}\left[t-\dfrac{\in}{\omega}\cos\omega t+\dfrac{\in}{\omega}\right]\right)^{\frac{1}{2}}$.

Using Eq. (5.10) in Eq. (5.9), we obtain

$$T_1(x,t)=\mu\left\{\frac{q^2}{k\gamma}(1+\in\sin\omega t)^2 s_0^{-1}\right\}\frac{x^2}{2}+\mu\left\{\frac{q}{k}\omega\in\cos\omega t\, s_0\right\}\frac{x^2}{2}-\mu\left\{\frac{q}{k}\omega\in\cos\omega t\right\}\frac{x^3}{6}, \tag{5.11}$$

$$T_2(x,t) = T_1(x,t) - \frac{\alpha\mu^2 q^2 (1+\in \sin \omega t)^2 s_0^{-1}}{k\gamma}\frac{x^2}{2} - \frac{\alpha\mu^2 q\omega \in \cos\omega t\, s_0}{k}\frac{x^2}{2}$$
$$+\frac{\alpha\mu^2 q\omega \in \cos\omega t}{k}\frac{x^3}{6} + \frac{\mu^2 q^2}{k\gamma}\left\{-\frac{q}{\gamma}(1+\in \sin\omega t)^3 s_0^{-3} + 2(1+\in \sin\omega t)\omega \in s_0^{-1}\cos\omega t\right\}\frac{x^4}{24}$$
$$+\frac{\mu^2 q}{k}\left\{\frac{\omega q}{\gamma}\in \cos\omega t(1+\in \sin\omega t)s_0^{-1} - (\omega^2 \in \sin\omega t)s_0\right\}\frac{x^4}{24} + \frac{\mu^2 q\omega^2 \in \sin\omega t}{k}\frac{x^5}{120},$$

(5.12)

and similarly, other components of $T(x,t)$ can be calculated.

Now, the solution $T(x,t)$ to the problem can be given by:

$$T(x,t) = T_0(x,t) + T_1(x,t) + T_2(x,t) + \cdots. \quad (5.13)$$

Now, by choosing the following linear and nonlinear operators, we have

$$L[\psi(t;p)] = \frac{d\psi(t;p)}{dt} \quad (5.14)$$

and

$$N[\psi(t;p)] = k\frac{\partial T(\psi(t;p),t)}{\partial x} + \gamma\psi(t;p)\frac{d\psi(t;p)}{dt}. \quad (5.15)$$

We construct the following homotopy for Eq. (5.4):

$$(1-p)[\psi(t;p) - s_0(t)] = p\hbar N[\psi(t;p)]. \quad (5.16)$$

From Eq. (5.16), we can easily find

$$\psi(t;0) = s_0 \quad (5.17)$$

and

$$\psi(t;1) = s(t). \quad (5.18)$$

According to Liao (2009) and Abbasbandy (2006), the *m*-th order deformation equation in context of Eq. (5.4) is:

$$L[s_m(t) - \chi_m s_{m-1}(t)] = \hbar N[s_{m-1}(t)]. \tag{5.19}$$

By considering the expression of s_0 (initial approximation for moving interface) and Eqs. (5.13), (5.17) and (5.19), the various components of $s(t)$, i.e. $s_1(t), s_2(t), \cdots$, can be calculated.

Hence, the approximate solution for $s(t)$ is given by

$$s(t) = s_0(t) + s_1(t) + \cdots. \tag{5.20}$$

5.4 Comparisons and Discussion

To show the accurateness of the obtained solution, we discuss the comparisons of our results for temperature profile $T(x,t)$ and the location of moving phase front $s(t)$ with the exact solution at $\in = 0$ through Tables 5.1 and 5.2, respectively. In case of $\in = 0$, the Eqs. (5.1)-(5.5) become a shoreline problem with a fixed line flux and a constant ocean level (Voller et al., 2004). In this chapter, the comparisons of our calculated results have been made with the exact solution established by Voller et al. (2004). Table 5.1 represents relative errors of temperature distribution between obtained results and exact result (given in Voller et al. (2004)) at α =1, $\in = 0$, k =1, $\mu = -1$ and $t = 5.5$. The absolute errors and relative errors of moving phase front are depicted in Table 5.2 at α =1, $\in = 0$, $\hbar = 1$ and k =1. From both the tables, it is clear that the obtained computational results agree well with the result of exact solution.

q	x	$T_N(x,t)$	$T_E(x,t)$	Absolute Error	Relative Error
0.5	0.1	0.212321	0.211090	1.20 e-03	5.80 e-03
	0.2	0.162679	0.160212	2.40 e-03	1.50 e-02
	0.3	0.113274	0.109579	3.60 e-03	3.30 e-02
	0.4	0.064106	0.059189	4.90 e-03	8.30 e-02
	0.5	0.015176	0.009037	6.10 e-03	6.70 e-02
1.0	0.1	0.641957	0.637125	4.80 e-03	7.50 e-03
	0.2	0.542968	0.533223	9.70 e-03	1.80 e-02
	0.3	0.444652	0.430042	1.40 e-02	3.30 e-02
	0.4	0.347007	0.327569	1.90 e-02	5.90 e-02
	0.5	0.250031	0.225792	2.40 e-02	1.00 e-01
1.5	0.1	1.213060	1.202430	1.00 e-02	8.80 e-03
	0.2	1.064920	1.043280	2.10 e-02	2.00 e-02
	0.3	0.918012	0.885505	3.20 e-02	3.60 e-02
	0.4	0.772339	0.729075	4.30 e-02	5.90 e-02
	0.5	0.627896	0.573966	5.30 e-02	9.30 e-02

Table 5.1. Comparison between exact value $T_E(x,t)$ and numerical value $T_N(x,t)$ of temperature distribution at $\gamma = 20$.

q	t	$s_N(t)$	$s_E(t)$	Absolute Error	Relative Error
0.5	1	0.199681	0.198055	1.60 e-03	8.20 e-03
	2	0.282205	0.280092	2.10 e-03	7.50 e-03
	3	0.345453	0.343041	2.40 e-03	7.00 e-03
	4	0.398724	0.396109	2.60 e-03	6.60 e-03
	5	0.445619	0.442864	2.70 e-03	6.20 e-03
1.0	1	0.281571	0.277484	4.00 e-03	1.40 e-02
	2	0.397457	0.392422	5.00 e-03	1.20 e-02
	3	0.486084	0.480616	5.40 e-03	1.10 e-02
	4	0.560600	0.554968	5.60 e-03	1.00 e-02
	5	0.626098	0.620473	5.60 e-03	0.90 e-02
2.0	1	0.394948	0.385578	9.30 e-03	2.40 e-02
	2	0.555582	0.545290	1.02 e-04	1.80 e-02
	3	0.677665	0.667841	9.80 e-03	1.40 e-02
	4	0.779793	0.771156	8.60 e-03	1.10 e-02
	5	0.869169	0.862179	6.90 e-03	0.80 e-02

Table 5.2. Comparison between exact value $s_E(t)$ and numerical value $s_N(t)$ of moving interface at $\gamma = 25$.

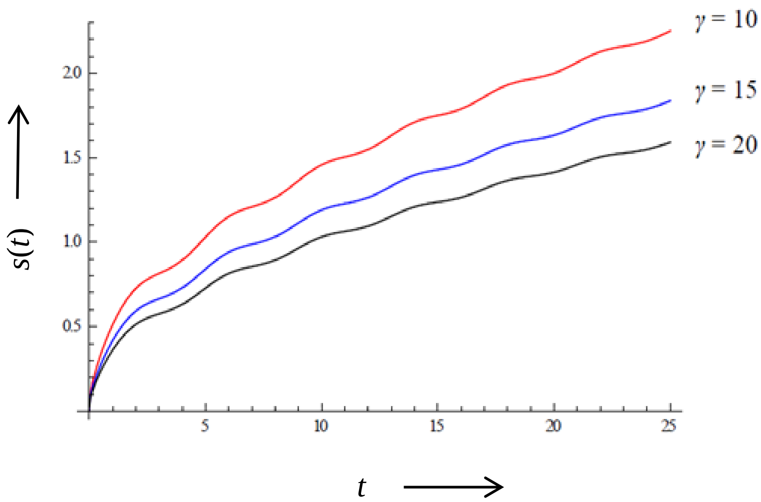

Fig.5.1. Plot of $s(t)$ vs. t at $\alpha = 1.0, q = 1.0, \in = 0.5$ and $\omega = \pi / 2$.

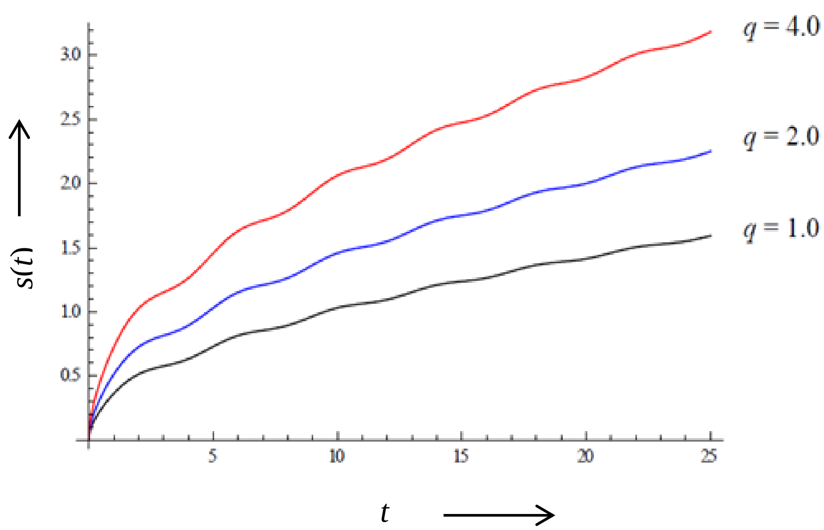

Fig.5.2. Plot of $s(t)$ vs. t at $\alpha = 1.0, \gamma = 20, \in = 0.5$ and $\omega = \pi / 2$.

Figs. 5.1 and 5.2 show the evolution of movement of phase front at the fixed value of thermal diffusivity ($\alpha = 1.0$), oscillation amplitude ($\in = 0.5$), $\hbar = 1$ and oscillation frequency ($\omega = \pi / 2$). In Figs. 5.1 and 5.2, the effect of periodic heat flux on the movement of phase front is depicted for different values of γ and *q*, respectively. From Fig. 5.1, it can be seen that phase front propagates periodically and the movement of phase front becomes slow when we enhance the parameter γ . However, Fig. 5.2 depicts that the periodic propagation of moving boundary $s(t)$ which becomes fast as the value of q rises. It is also observed that when we raise the value of q , it makes melting/freezing process fast.

5.5 Conclusion

In this work, we study a complicated phase-change problem with periodic heat flux and variable latent heat term. As per authors' knowledge, the exact solution to the proposed problem is not available in literature yet. Therefore, homotopy analysis technique has been used to get an approximate analytical solution to the problem, and we have seen that our computed results are sufficiently close to the analytical solution when the surface heat flux is a constant, i.e. the oscillation amplitude is zero. In this chapter, we have seen that the movement of interface/phase front is profoundly affected due to the change in various parameters, like oscillation amplitude, oscillation frequency, γ and *q*. It is also seen that the homotopy analysis technique is a straight forward method. Moreover, this technique is sufficiently accurate and efficient to solve different types of phase-change problems arising in the various industries.

*****